Hindawi
Journal of Chemistry
Volume 2021, Article ID 5589837, 16 pages
https://doi.org/10.1155/2021/5589837

Research Article

A Four-Component Domino Reaction: An Eco-Compatible and Highly Efficient Construction of 1,8-Naphthyridine Derivatives, Their *In Silico* Molecular Docking, Drug Likeness, ADME, and Toxicity Studies

Ankita Garg, Aschalew Tadesse, and Rajalakshmanan Eswaramoorthy

Department of Applied Chemistry, School of Applied Natural Science, Adama Science and Technology University, Adama, P.O. 1888, Ethiopia

Correspondence should be addressed to Rajalakshmanan Eswaramoorthy; rajalakshmanan.e@gmail.com

Received 15 February 2021; Revised 3 March 2021; Accepted 16 March 2021; Published 31 March 2021

Academic Editor: Simone Carradori

A multicomponent domino reaction of enaminone, malononitrile, and *o*-phthalaldehyde has been established, providing direct access to novel highly functionalized pentacyclic cyclopenta [b] indeno [1, 2, 3-de] [1,8] naphthyridine derivatives. The simplicity of execution, readily available substrates, high yields, excellent functional group tolerance, scalability, and good scores of environmental parameters make this synthetic strategy more sustainable and worthy of further attention. This one-pot transformation, which involved multiple steps and did not require the use of a catalyst, constructed four new C-C bonds, two new C-N bonds, and three new rings, with efficient use of all reactants. Furthermore, we performed *in silico* molecular docking analysis for prediction of anticancer (against human topoisomerase IIβ protein) and antimicrobial (against *E.coli.* DNA gyrase B protein) activities. Drug likeness and ADMET studies were also predicted. Overall investigation indicates that compound 6i may serve as a candidate that could be developed as potential anticancer and antimicrobial agent among all.

1. Introduction

The naphthyridine framework exists in a number of natural and synthetic substances with various chemical reactivities and exceptional physicochemical [1] and biological properties [2, 3], which include anticancer, [4] HIV-I inhibitor, [5] anticonvulsant, [6] antimalarial [7], and anti-Alzheimer [8]. Among the six possible (1,5–, 1,6–, 1,7–, 1,8–, 2,6–, and 2,7–) isomeric pyridopyridines, [9, 10] 1,8-naphthyridines and their derivatives have diverse potential in clinical and medicinal chemistry due to their anti-inflammatory, [11] antimalarial, [12] antihypertensive, [13] gastric antisecretory, [14] antiplatelet aggregation, [15] AChE inhibitory, [16] antihistaminic, [2] antimicrobial [17, 18], and anticancer [19–21] activities (Figure 1). Additionally, they have potential in physical chemistry as fluorescent sensors [22]. These compounds have been investigated as potential anticancer agents, and several compounds are part of clinical trials. Moreover, it has been reported that few 1,8-naphthyridine derivatives (e.g., Vosaroxin, Figure 1) were found to inhibit topoisomerase II and displayed potent anticancer activity. Vosaroxin (formerly voreloxin) is a first-in-class anticancer agent that intercalates DNA and inhibits topoisomerase II, inducing site-selective double-strand breaks (DSB), G2 arrest, and apoptosis [23, 24]. Chemical modifications of the naphthyridine ring, including conversion into other similar ring systems, have been known to increase the anticancer activity of these compounds [21, 25–27].

Nevertheless, the true potential of this nitrogen containing heterocyclic framework has largely remained untapped owing to a lack of general diversity-oriented synthetic strategies. In the last two decades, growing concern about the environment has forced chemists to develop novel and sustainable chemical processes through the principles of "green chemistry" [28, 29]. As a consequence, synthetic protocols that allow diversity and are operationally simple,

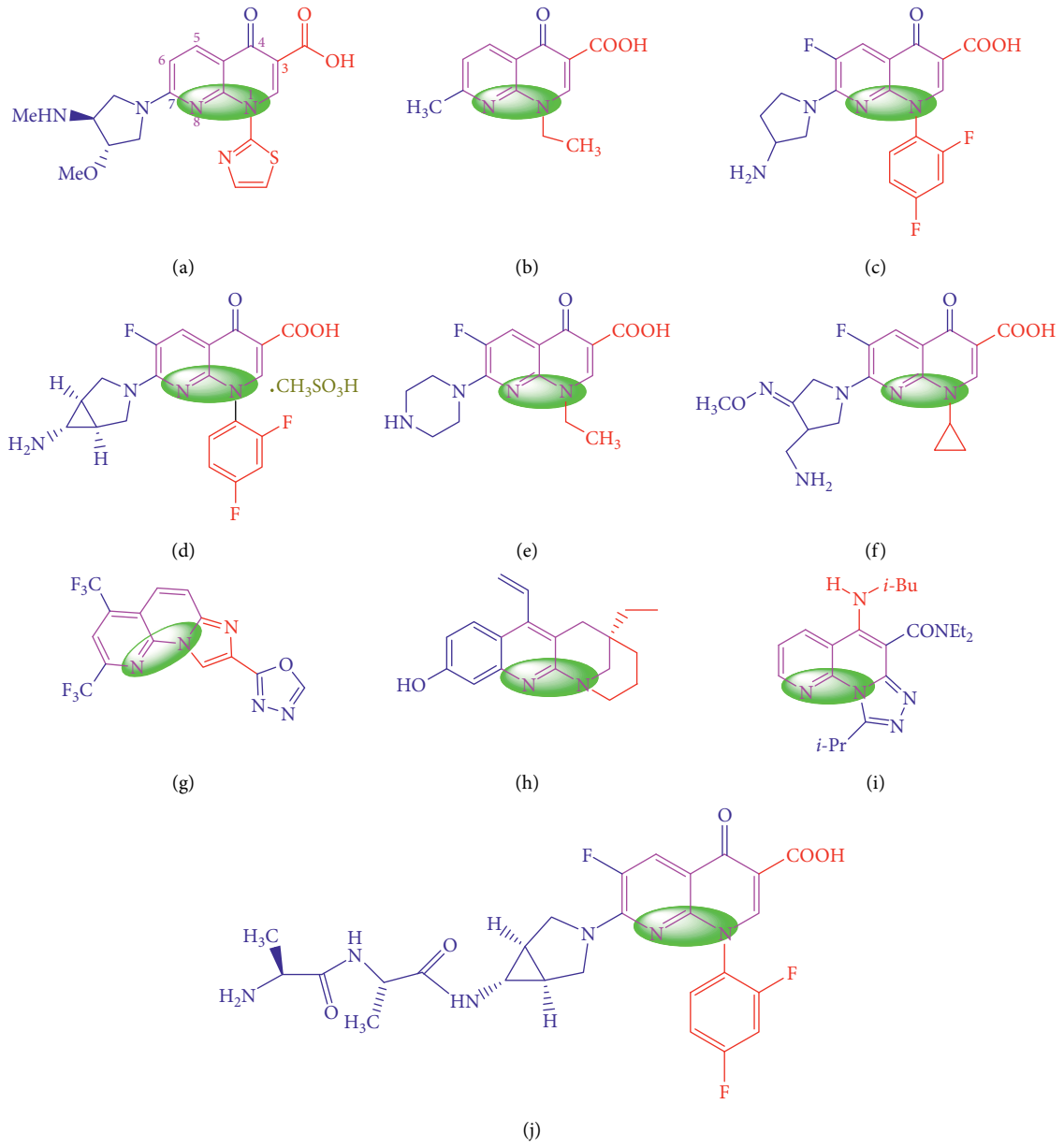

Figure 1: Available drugs having 1,8-naphthyridine nucleus. (a) Vosaroxin. (b) Nalidixic acid. (c) Tosufloxacin. (d) Trovafloxacin mesylate. (e) Enoxacin. (f) Gemifloxacin. (g) RO8191. (h) Eucophylline. (i) NF_{161}. (j) Alatrofloxacin.

mild, step-economical, high yielding, and compatible with green solvents are of prime importance [28, 29]. To achieve these goals, multicomponent domino reactions (MDRs) come into play [30–32]. Significantly, MDRs enable assembly of three or more reactants in a single and an ordered event to render intricate and complex heterocyclic entities in an atom-and step-economical manner [33, 34].

To date, the synthesis of 1,8-naphthyridine derivatives has been achieved via a variety of approaches including the condensation of 2-aminopyridine derivatives with carbonyl compounds under Conrad-Limpach, [35] Skraup, [36], and Friedlander [37] reaction conditions. The above methods suffer from the use of corrosive reagents, poor yields, multistep syntheses, and harsh reaction conditions. More importantly, all the reported methods need expensive and rare starting materials, the synthesis of which may demand significant scientific investment in itself. In the above light, a catalyst-free MDR-based route towards the assembly of novel pentacyclic cyclopenta [b] indeno [1, 2, 3-de] [1, 8] naphthyridine derivatives starting from cheap and abundantly available starting materials would be of great significance from both an economical and a chemical standpoint.

In continuation to our ongoing endeavors to prepare novel biologically active nitrogen containing heterocyclic entities, by using green and benign MCR protocols, [38, 39] we herein report a domino four-component strategy for the efficient synthesis of highly functionalized pentacyclic

cyclopenta [b] indeno [1, 2, 3-de] [1,8] naphthyridine derivatives by utilizing cheap and commercially available reagents, that is, different enaminones, malononitrile, and *o*-phthalaldehyde under appropriate catalyst-free and mild microwave conditions (Scheme 1). Many chemical modifications have been carried out previously also at N-1, C-5, C-6, C-7, and C-3 positions, [21, 25–27] but this work represents a novel synthetic methodology as well as designing strategy to find out less toxic and potent anticancer agents.

The pharmacokinetics (PK) and pharmacodynamics (PD) evaluations play a crucial role in drug development [40, 41]. The evaluation of pharmacological parameters such as drug-likeness, ADME, and toxicity is paramount in identifying lead compounds [40, 41]. Recently, *in silico* methods that include molecular docking analysis and online ADMET predictions (SwissADME and ProTox-II) facilitate the process of identifying the potential molecule [41–45]. In this present investigation, we report a new green synthetic methodology and characterization of novel 1,8-naphthyridine derivatives and their *in silico* anticancer and antimicrobial molecular docking analysis and pharmacological properties predictions such as drug-likeness, ADME, and toxicity.

2. Materials and Methods

2.1. General. ^{1}H NMR and ^{13}C NMR spectra were recorded on Jeol Resonance ECX-400II (400 MHz). Chemical shifts (δ in ppm) and coupling constant (J in Hz) are calibrated relative to either internal solvent tetramethylsilane (TMS) ($\delta_H = 0.00$ ppm) or DMSO-d_6 ($\delta_H = 3.33$ ppm). In the ^{1}H NMR data, the following abbreviations were used throughout: s = singlet, d = doublet, t = triplet, dd = double doublets, m = multiplet, and brs = broad singlet. In the ^{13}C NMR spectra, chemical shifts are calibrated relative to DMSO-d_6 ($\delta_C = 39.51$ ppm). The High-Resolution Mass Spectra (HR-MS) were performed on Bruker Daltonics micrOTOF-QII® spectrometer using ESI ionization. IR spectra were recorded on PerkinElmer Spectrum Two FT-IR spectrometer. Melting points were performed with *OptiMelt* automated melting point system.

The reactions were performed in a G-10 Borosilicate glass vial sealed with Teflon septum in Anton Paar Monowave 300 reactor®, operating at a frequency of 2.455 GHz with continuous irradiation power of 0 to 300 W. Analysis of the reactions was done by thin layer chromatography (TLC) on Merck precoated silica gel TLC plates (Merck® $60F_{254}$). Chemicals and reagents were purchased from Sigma-Aldrich and Alfa Aesar. All solvents, ethanol, petroleum ether, and ethyl acetate, were purchased from locally available commercial sources and used as received.

2.2. Synthesis

2.2.1. General Procedure for the Synthesis of Synthons (Enaminones) (3a-i). A mixture of cyclopentane-1, 3-dione 1 (1.0 mmol), and the suitable amine 2 (2.0 mmol) was introduced in a G-10 glass vial capped with a Teflon septum and was subjected to microwave irradiation with the initial ramp time of 1 minute at 60°C and then the temperature was raised to 160°C with a holding time of 10 minutes in neat. The reaction was monitored by TLC. Synthons 3a-i were obtained for further use in the synthesis of final products 6a-i. All synthons 3a-i were characterized by ^{1}H NMR and ^{13}C NMR spectroscopies.

2.2.2. General Procedure for the Synthesis of Products (6a-i). A mixture of enaminone 3 (1.0 mmol), malononitrile 4 (2.2 mmol, 2.2 equiv), and *o*-phthalaldehyde 5 (1.0 mmol) was introduced in a G-10 glass vial capped with a Teflon septum and was subjected to microwave irradiation with the initial ramp time of 1 minute at 60°C and then the temperature was raised to 110°C with a holding time of 20 minutes with DMF (2 mL) as a solvent. The reaction was monitored by TLC. After the completion, the reaction mixture was then cooled to room temperature and diluted with cold water (40 mL) and then filtered; the precipitate was collected and purified by recrystallization from 95% EtOH except 6h which was purified by silica gel column chromatography (eluent 15–20% ethyl acetate/pet. ether). The analytical data for representing compounds are shown below.

(1) *6-Amino-1-oxo-1,2,3, 4,7a,11b-hexahydro-4a1H-cyclopenta [b] Indeno [1, 2, 3-de] [1, 8] Naphthyridine-4a1,7-dicarbonitrile (6a)*. Yellow solid (89%), 274–276°C; IR (KBr) (4000–600 cm^{-1}): ν_{max}: 3349, 3334, 2960, 2172, 1657, 1628, 1558, 1490, 1378, 1202, 1045, 732, 696. ^{1}H NMR: (400 MHz, DMSO-d_6) δ 2.44 (s, 4H), 4.68 (s, 1H), 4.81 (s, 1H), 6.67 (s, 2H), 7.24–7.42 (m, 4H), 9.22 (brs, NH) ppm. ^{13}C NMR: (100 MHz, DMSO-d_6) δ 26.8, 34.2, 42.7, 46.2, 49.1, 52.8, 115.2, 117.4, 129.2, 129.4, 129.7, 130.0, 130.4, 140.9, 141.3, 154.1, 157.1, 167.8, 202.1 ppm. HR-MS (ESI) for $C_{19}H_{13}N_5O$ m/z calcd.: 328.1154; found: 328.1152 $[M + H]^+$.

(2) *6-Amino-1-oxo-4-phenyl-1,2,3,4,7a,11b-hexahydro-4a1H-cyclopenta [b] Indeno [1, 2, 3-de] [1, 8] Naphthyridine-4a1,7-dicarbonitrile (6b).* Yellow solid (92%), 278–280°C; IR (KBr) (4000–600 cm^{-1}): ν_{max}: 3339, 2957, 2174, 1621, 1591, 1470, 1348, 1278, 1188, 1045, 764, 688. ^{1}H NMR: (400 MHz, DMSO-d_6) δ 2.46 (s, 4H), 4.68 (s, 1H), 4.81 (s, 1H), 6.67 (s, 2H), 7.015 (dd, 2H, $J = 20$ & 8 Hz), 7.22–7.43 (m, 6H), 7.51 (t, 1H, $J = 8$ Hz) ppm. ^{13}C NMR: (100 MHz, DMSO-d_6) δ 26.5, 34.3, 42.8, 46.3, 49.1, 52.6, 115.2, 117.4, 122.0, 123.4, 123.6, 127.9, 129.2, 129.4, 129.7, 130.0, 130.4, 134.3, 137.3, 141.1, 141.4, 154.1, 157.2, 167.9, 202.3 ppm. HR-MS (ESI) for $C_{25}H_{17}N_5O$ m/z calcd.: 404.1467; found: 404.1471 $[M + H]^+$.

(3) *6-Amino-4-(4-methoxyphenyl)-1-oxo-1,2,3,4,7a,11b-hexahydro-4a1H-cyclopenta [b] Indeno [1, 2, 3-de] [1, 8] Naphthyridine-4a1,7-dicarbonitrile (6c).* Yellow solid (93%), >300°C; IR (KBr) (4000–600 cm^{-1}): ν_{max}: 3336, 2954, 1662, 1589, 1382, 1336, 1248, 1125, 1009, 879, 742, 605. ^{1}H NMR: (400 MHz, DMSO-d_6) δ 3.72 (s, 4H), 4.115 (q, 3H, $J = 8$ Hz), 4.66 (s, 1H), 4.78 (s, 1H), 6.66 (s, 2H), 6.90 (s, 2H), 7.03 (d, 2H, $J = 8$ Hz), 7.13 (d, 1H, $J = 8$ Hz), 7.23–7.36 (m, 3H) ppm. ^{13}C NMR: (100 MHz, DMSO-d_6) δ 27.1, 29.8, 34.7, 43.2, 46.9, 49.6, 53.4, 115.2, 117.7, 123.0, 123.4, 123.6, 125.0, 127.9, 128.5, 130.0, 130.1, 130.4, 137.6, 140.3, 140.9, 141.3, 154.7, 157.4, 168.5, 202.3 ppm.

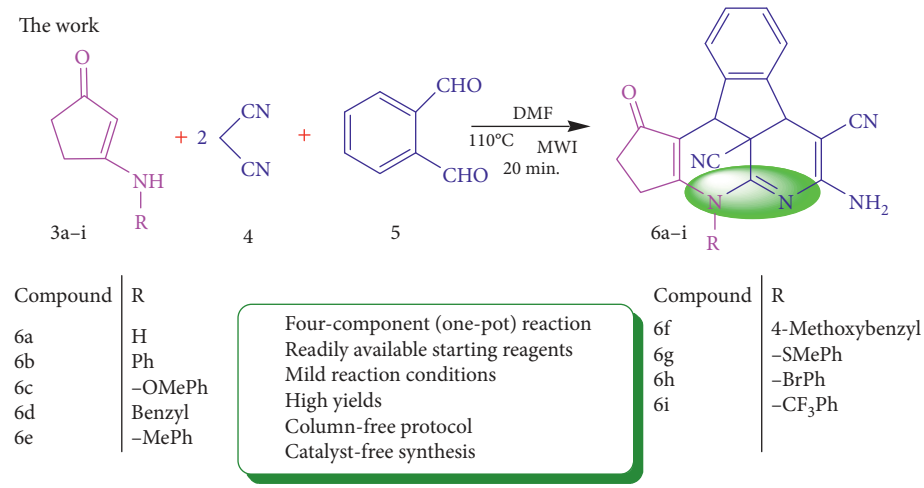

Scheme 1: Microwave-assisted domino protocol for the synthesis of cyclopenta [b] indeno [1, 2, 3-de] [1,8] naphthyridine derivatives.

HR-MS (ESI) for $C_{26}H_{19}N_5O_2$ m/z calcd.: 434.1572; found: 434.1568 $[M+H]^+$.

(4) *6-Amino-4-benzyl-1-oxo-1,2,3,4,7a,11b-hexahydro-4a1H-cyclopenta [b] Indeno [1, 2, 3-de] [1, 8] Naphthyridine-4a1,7-dicarbonitrile (6d)*. Yellow solid (82%), 275–278°C; IR (KBr) (4000–600 cm^{-1}): ν_{max}: 3331, 2958, 2174, 1654, 1631, 1564, 1451, 1338, 1258, 1212, 1168, 735. ^{1}H NMR: (400 MHz, DMSO-d_6) δ 2.47 (s, 4H), 4.06 (s, 2H), 4.68 (s, 1H), 4.85 (s, 1H), 6.67 (s, 2H), 7.04 (d, 2H, $J = 8$ Hz) 7.22–7.42 (m, 6H), 7.51–7.56 (m, 1H) ppm. ^{13}C NMR: (100 MHz, DMSO-d_6) δ 26.5, 31.6, 42.5, 44.6, 46.1, 48.9, 52.6, 115.2, 115.6, 117.4, 121.8, 123.8, 127.9, 129.0, 129.4, 130.0, 130.4, 130.8, 137.3, 140.3, 140.9, 141.3, 154.1, 157.1, 167.8, 202.1 ppm. HR-MS (ESI) for $C_{26}H_{19}N_5O$ m/z calcd.: 418.1623; found: 418.1634 $[M+H]^+$.

(5) *6-Amino-1-oxo-4-(p-tolyl)-1,2,3,4,7a,11b-hexahydro-4a1H-cyclopenta [b] Indeno [1, 2, 3-de] [1, 8] Naphthyridine-4a1,7-dicarbonitrile (6e)*. Yellow solid (88%), >300°C; IR (KBr) (4000–600 cm^{-1}): ν_{max}: 3419, 2954, 2161, 1632, 1605, 1565, 1470, 1380, 1283, 1222, 935, 849, 736, 688. ^{1}H NMR: (400 MHz, DMSO-d_6) δ 3.1325 (dd, 3H, 32 & 16 Hz), 3.72 (s, 4H), 4.66 (s, 1H), 4.78 (s, 1H), 6.66 (s, 2H), 6.97 (s, 2H), 7.02–7.39 (m, 6H) ppm. ^{13}C NMR: (100 MHz, DMSO-d_6) δ 20.1, 26.8, 34.2, 42.7, 46.2, 49.1, 52.8, 115.2, 117.4, 121.8, 123.4, 123.6, 127.9, 129.2, 129.4, 129.7, 130.0, 130.4, 137.4, 139.4, 141.1, 141.4, 155.5, 158.8, 170.1, 200.0 ppm. HR-MS (ESI) for $C_{26}H_{19}N_5O$ m/z calcd.: 418.1623; found: 418.1618 $[M+H]^+$.

(6) *6-Amino-4-(4-methoxybenzyl)-1-oxo-1,2,3,4,7a,11b-hexahydro-4a1H-cyclopenta [b] Indeno [1, 2, 3-de] [1, 8] Naphthyridine-4a1,7-dicarbonitrile (6f)*. Yellow solid (81%), 284–286°C; IR (KBr) (4000–600 cm^{-1}): ν_{max}: 3330, 2961, 2181, 1661, 1568, 1467, 1332, 1247, 1188, 1045, 995, 764, 732. ^{1}H NMR: (400 MHz, DMSO-d_6) δ 3.72 (s, 4H), 3.88 (d, 2H, 8 Hz), 4.105 (q, 3H, $J = 12$ Hz), 4.66 (s, 1H), 4.82 (s, 1H), 6.62 (s, 2H), 6.93 (m, 2H), 7.13 (d, 2H, $J = 8$ Hz), 7.17–7.39 (m, 4H) ppm. ^{13}C NMR: (100 MHz, DMSO-d_6) δ 26.8, 30.4, 33.9, 46.0, 49.1, 52.8, 55.3, 58.2, 115.2, 115.6, 117.4, 120.7, 121.8, 123.0, 123.4, 123.6, 129.2, 129.4, 129.7, 130.0, 137.3, 140.9, 141.3, 154.7, 157.2, 167.5, 202.2 ppm. HR-MS (ESI) for $C_{27}H_{21}N_5O_2$ m/z calcd.: 448.1729; found: 448.1734 $[M+H]^+$.

(7) *6-Amino-4-(4-(methylthio)phenyl)-1-oxo-1,2,3,4,7a,-11b-hexahydro-4a1H-cyclopenta [b] Indeno [1, 2, 3-de] [1, 8] Naphthyridine-4a1,7-dicarbonitrile (6g)*. Yellow solid (75%), >300°C; IR (KBr) (4000–600 cm^{-1}): ν_{max}: 3328, 2956, 2180, 1633, 1563, 1509, 1467, 1382, 1251, 1188, 997, 767, 647, 610. ^{1}H NMR: (400 MHz, DMSO-d_6) δ 2.38–2.59 (m, 3H), 3.72 (s, 4H), 4.66 (s, 1H), 4.78 (s, 1H), 6.62 (s, 2H), 6.90 (s, 2H), 7.03 (d, 2H, $J = 8$ Hz), 7.12–7.34 (m, 4H) ppm. ^{13}C NMR: (100 MHz, DMSO-d_6) δ 17.8, 26.5, 34.5, 43.4, 46.6, 49.5, 53.5, 115.2, 117.4, 121.8, 123.0, 123.4, 123.6, 127.9, 129.2, 129.4, 129.7, 130.0, 130.4, 137.3, 140.9, 141.3, 154.1, 157.1, 167.8, 202.1 ppm. HR-MS (ESI) for $C_{26}H_{19}N_5OS$ m/z calcd.: 450.1344; found: 450.1349 $[M+H]^+$.

(8) *6-Amino-4-(4-bromophenyl)-1-oxo-1,2,3,4,7a,11b-hexahydro-4a1H-cyclopenta [b] Indeno [1, 2, 3-de] [1, 8] Naphthyridine-4a1,7-dicarbonitrile (6h)*. Yellow solid (74%), >300°C; IR (KBr) (4000–600 cm^{-1}): ν_{max}: 3335, 2963, 2176, 1659, 1629, 1568, 1504 1379, 1246, 1189, 991, 842, 739. ^{1}H NMR: (400 MHz, DMSO-d_6) δ 2.46 (s, 4H), 4.93 (s, 1H), 5.08 (s, 1H), 6.49 (s, 2H), 6.90 (s, 2H), 7.03 (d, 2H, $J = 8$ Hz), 7.12–7.34 (m, 4H) ppm. ^{13}C NMR: (100 MHz, DMSO-d_6) δ 24.6, 32.0, 46.0, 49.2, 52.9, 57.0, 115.2, 117.4, 121.8, 123.4, 123.6, 127.9, 129.2, 129.4, 129.7, 130.0, 130.4, 130.6, 137.3, 140.9, 141.3, 157.2, 159.8, 170.5, 204.5 ppm. HR-MS (ESI) for $C_{25}H_{16}BrN_5O$ m/z calcd.: 483.0518; found: 483.0512 $[M+H]^+$.

(9) *6-Amino-1-oxo-4-(4-trifluoromethyl)phenyl)-1,2,-3,4,7a,11b-hexahydro-4a1H-cyclopenta [b] Indeno[1, 2, 3-de] [1, 8] Naphthyridine-4a1,7-dicarbonitrile (6i)*. Yellow solid (72%), 284–286°C; IR (KBr) (4000–600 cm^{-1}): ν_{max}: 3339, 2960, 2174, 1621, 1593, 1457, 1385, 1275, 1128, 998, 732, 616. ^{1}H NMR: (400 MHz, DMSO-d_6) δ 3.72 (s, 4H), 4.66 (s, 1H), 4.78 (s, 1H), 6.40 (s, 2H), 6.66 (s, 2H), 6.74–6.81 (m, 2H), 7.12–7.34 (m, 4H) ppm. ^{13}C NMR: (100 MHz, DMSO-d_6) δ 24.6, 32.0, 46.0, 49.2, 52.9, 57.0, 97.1, 115.2, 117.4, 121.8, 123.4, 123.6, 127.9, 129.2, 129.4, 129.7, 130.0, 130.4, 130.6, 137.3, 140.9, 141.3, 157.2, 159.8, 170.5, 204.5 ppm. HR-MS

(ESI) for $C_{26}H_{16}F_3N_5O$ m/z calcd.: 472.1340; found: 472.1352 $[M+H]^+$.

2.3. In Silico Molecular Docking Methodology

2.3.1. Preparation of Ligands. The 2D structures (.mol) of all synthesized compounds (6a-i) were drawn and each individual structure was analyzed by using ChemDraw 16.0. All the compounds (6a-i) were converted to 3D structure (.pdb) using Chem3D 16.0. The 3D coordinates (.pdb) of each molecule were loaded onto Chem3D for energy minimization.

2.3.2. Preparation of Macromolecule. The crystal structures of receptor molecule *E. coli* gyrase B (PDB ID: 6F86) and human topoisomerase IIβ with DNA (PDB ID 3QX3) were downloaded from protein data bank. The protein preparation was done using the reported standard protocol by removing the cocrystallized ligand, selected water molecules, and cofactors, and the target protein file was prepared by leaving the associated residue with protein by using autopreparation of target protein file AutoDock 4.2 (MGLTools 1.5.7).

2.3.3. AutoDock Vina Analysis. The graphical user interface program AutoDock 4.2 was used to set the grid box for docking simulations. The grid was set so that it surrounds the region of interest in the macromolecule. The docking algorithm provided with AutoDock Vina was used to search for the best docked conformation between ligand and protein. During the docking process, a maximum of nine conformers were considered for each ligand. The conformations with the most favorable (least) free binding energy were selected for analyzing the interactions between the target receptor and ligands by Discovery Studio Visualizer and PyMOL.

AutoDock Vina with standard protocol was used to dock the proteins (PDB ID: 6F86 and 3QX3) and synthesized novel 1,8-naphthyridine ligands (6a-i) into the active site of proteins. The molecular docking studies were carried out using AutoDockTools (ADT) [44], which is a free graphic user interface (GUI) for the AutoDock Vina program. The grid box was constructed using $15 \times 15 \times 15$, pointing in x, y, and z directions, respectively, with a grid point spacing of 0.375 Å. The center grid box is of $35.58 \times 95.63 \times 52.38$ Å and $62 \times 30 \times 62$ Å for 3QX3 and 6F86, respectively. Nine different conformations were generated for each ligand scored using AutoDock Vina functions and were ranked according to their binding energies. The ligands are represented in different color, and H-bonds and the interacting residues are represented in stick model representation.

2.3.4. In Silico Pharmacokinetics and Toxicity. Drug-likeness is a prediction that determines whether a particular pharmacological agent has properties consistent with being an orally active drug. The chemical structure of the compounds (6a-i) was converted to their canonical simplified molecular input line entry (SMILE) system and submitted to SwissADME tool to estimate *in silico* pharmacokinetic parameters. SwissADME predictor provides information on the numbers of hydrogen donors, hydrogen acceptors, and rotatable bonds, as well as total polar surface area of a compound. The ligands were also subjected to Lipinski et al., screened using SwissADME and PreADMET predictors. The organ toxicities and toxicological endpoints of the ligands and their LD_{50} were predicted using ProTox-II and OSIRIS Property Explorer [42, 43]. The analyses of the compounds were compared with that of Vosaroxin, a clinical-trial phase III drug.

3. Results and Discussion

3.1. Chemistry. A series of novel 1,8-naphthyridine derivatives are synthesized via a four-component domino reaction with no more than 20 minutes of microwave irradiation. This one-pot transformation, which involved multiple steps and did not require the use of a catalyst, constructed four new C-C bonds, two new C-N bonds, and three new rings with efficient use of all reactants, which are readily available and cheap. Moreover, the proposed strategy involves neither tedious workup nor column purification steps. Furthermore, the methodology has excellent green credentials, scoring well in a number of green metrics, hence showing this approach to be an ideal green and sustainable process even at gram scale.

Furthermore, it is noteworthy that we synthesized the starting material enaminone (3a-i) under microwave irradiation, starting with cyclopentane-1, 3-dione (1), and various amines (2a-i) in neat (catalyst- and solvent-free conditions) at 160°C for 10 min. The reaction and products are summarized in Scheme 2. This work represents the first example of synthesizing different enaminones through this simple and green methodology. Hence, synthesis of compounds (3a-i) was accomplished with readily available ammonium acetate (2a) aromatic or benzylic amines (2b-i) and the commercially available cyclopentane-1,3-dione.

After synthesis of synthons 3a-i, we further used a 1:2:1 mixture of 3-aminocyclopent-2-enone (3a), malononitrile (4), and *o*-phthalaldehyde (5) in ethanol [46] at 100°C for 20 minutes under microwave irradiation, without using catalyst. Only 38% yield of the desired compound 6-amino-1-oxo-1, 2, 3, 4, 7a, 11b-hexahydro-4a1H-cyclopenta [b] indeno [1, 2, 3-de] [1,8] naphthyridine-4a1, 7-dicarbonitrile (6a) could be afforded. This synthesized 6a derivative was characterized using IR, ^{1}H NMR, ^{13}C NMR, and HR-MS spectroscopies (see supplementary data (Figures S1–S18)). Optimization data are shown in Table 1. The addition of catalysts such as L-proline [47], piperidine [48], p-toluenesulfonic acid, [49] and silica sulfuric acid [50] did not improve the yields (Table 1, entries 2–5). DMF [51] was chosen as the solvent for all further reactions due to positive results. When the reaction was carried out at 90°C, 100°C, 110°C, and 120°C, 6a was obtained in yields of 70%, 75%, 89%, and 80% (Table 1, entries 6 and 11–13), respectively [52]. We checked the reaction with DMF at 110°C for 15 min., but it further reduced the yield and multiple spots

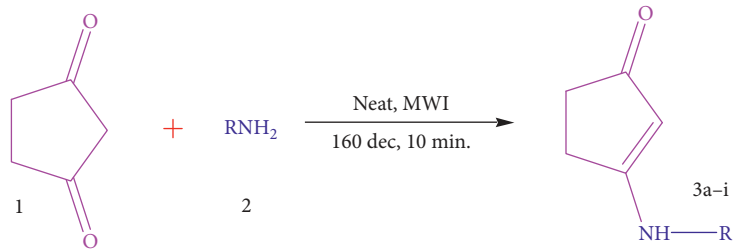

Compound	R	Yield %
3a	H	93
3b	Ph	89
3c	–OMePh	86
3d	Benzyl	85
3e	–MePh	91
3f	4-Methoxybenzyl	83
3g	–SMePh	88
3h	–BrPh	80
3i	$-CF_3Ph$	78

Scheme 2: Synthesis of compounds 3a-i under microwave irradiation.

Table 1: Optimization of reaction conditions for synthesis of 6a under microwave irradiation.

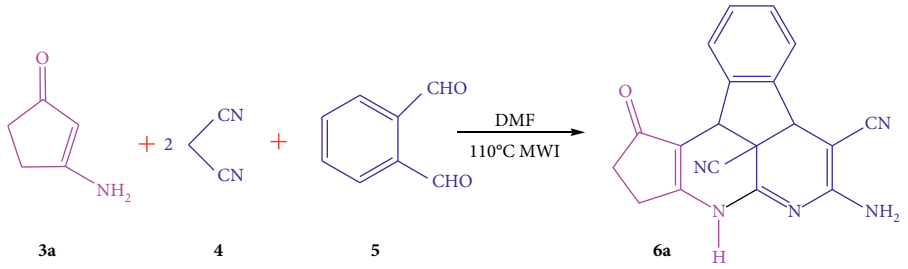

3a 4 5 6a

Entry	Solvent	Catalyst (mol %)	Temp. (°C)[a]	Time (min.)	Yield (%)[b]
1	EtOH	—	100	20	38
2	EtOH	L-Proline (15)	100	20	40
3	EtOH	p-TsOH (15)	100	20	Trace
4	EtOH	Piperidine (10)	100	20	Trace
5	EtOH	SSA (10)	100	20	Trace
6	DMF	—	100	20	75
7	CH3CN	—	100	20	10
8	CH3OH	—	100	20	5
9	OHCH2CH2OH	—	100	20	35
10	H2O	—	100	20	25
11	DMF	—	90	20	70
12	DMF	—	110	20	89
13	DMF	—	120	20	80
14	DMF	—	120	15	60

General conditions: 3-aminocyclopent-2-enone 3a (1 mmol); malononitrile 4 (2.2 mmol); phthaldialdehyde 5 (1 mmol); DMF (2 ml); [a]Anton Paar Monowave 300 reactor; irradiation power: 850 W; ramp time: 1 min; 60°C; [b]isolated yield by recrystallization.

appeared at TLC (Table 1, entry 14). These experiments showed that conditions of 110°C in DMF, without a catalyst, under microwave irradiation for 20 minutes provided the highest yield with column-free protocol. Using the optimal conditions, we investigated the substrate scope of the transformation. The results are summarized in Table 2. As shown in Table 2, phenyl groups bearing either electron-withdrawing or electron-donating groups on the enaminone ring as well as the unsubstituted enaminone as in the case of 6a were well tolerated under the reaction conditions, leading to the final products in satisfactory yields (82 ± 10%).

To conclude our analysis of this MDR, we have calculated green metrics [53, 54] comprising E-factor, atom economy (AE), process mass intensity (PMI), reaction mass efficiency (RME), and carbon efficiency (CE) for the process. Therefore, we carried out the reaction on a 2 mmol scale by reacting enaminone 3c (2 mmol, 0.407 g) and malononitrile 4 (4.4 mmol, 0.291 g) with *o*-phthalaldehyde 5 (2 mmol, 0.268 g) under the optimal conditions, which in turn provided 0.803 g of pure 6c in 90% yield (Table 3). The calculated green metrics for the above reaction (AE = 92.32 %, CE = 72.83 %, E-factor = 3.938, RME = 83.13%, and

Table 2: Synthesis and substrate scope of compounds 6a-i under microwave irradiation.

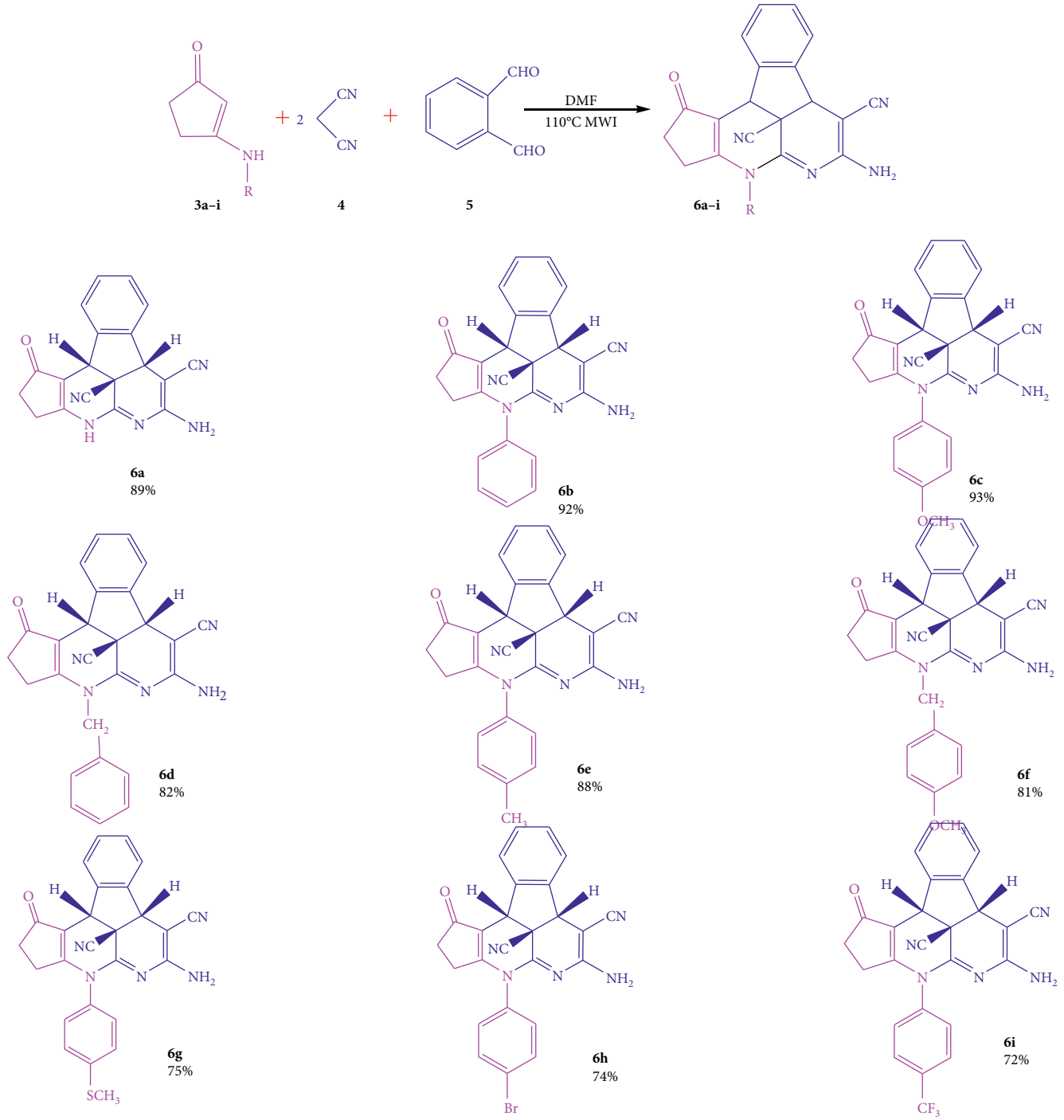

PMI = 4.938) establish the environment friendliness of the present method (see supplementary materials available here).

A proposed mechanism for this new four-component domino reaction is shown in Scheme 3. An initial Knoevenagel condensation [55, 56] of *o*-phthalaldehyde (5) with two malononitrile (4) molecules followed by Michael addition [57] of enaminone (3) with intermediate A proceeding towards cyclization and imine-enamine tautomerization to give product 6 has been predicted (see supplementary data available here).

A catalyst-free eco-friendly domino methodology towards the assembly of hexahydro-4a1H-cyclopenta [b] indeno [1, 2, 3-de] [1,8] naphthyridine-4a1,7-dicarbonitrile derivatives has been developed from commercially available cyclopentane-1, 3-dione, aromatic amine (2b-i) (or

ammonium acetate in case of 2a), malononitrile, and *o*-phthalaldehyde. The operational simplicity, readily available substrates, cheap reagents, high to excellent yields, and wide functional group tolerance are the key features of the present MDR protocol. The usefulness of these domino reactions is shown by the fact that up to six new bonds (four C-C bonds and two C-N bonds) and three new rings (a tricyclic 5-6-6 skeleton consisting of cyclopentene and two pyridines) were readily formed in domino fashion. This work represents the construction of these special types of polyhydronaphthyridine skeletons in one pot.

3.2. Molecular Docking Studies. Molecular docking studies are generally employed to investigate the binding energy and to further validate the molecular mechanisms for ligands at the active site of a protein. To understand the binding mode of 1,8-naphthyridine derivatives, all the synthesized compounds were subjected to molecular docking studies against selected proteins, namely, human topoisomerase IIβ and *E. coli*. DNA gyrase B using Autodock Vina [44].

3.2.1. Binding Mode of Analysis of Synthesized 1,8-Naphthyridine Derivatives Docked against Human Topoisomerase II Beta (PDB ID 3QX3). It has been reported that topoisomerase IIβ is one of the elucidated targets for antitumor agents such as 1,8-naphthyridine derivatives (e.g., Vosaroxin) [58, 59]. Therefore, in this study, the molecular docking analysis of the synthesized compounds (6a-i) was carried out to investigate their binding interaction within the binding sites of human topoisomerase IIβ and the results were compared with standard anticancer agent in class (Vosaroxin). The synthesized compounds (6a-i) were found to have minimum binding energy ranging from –6.2 to –6.7 kcal/mol (Table 4). Compared with Vosaroxin (–5.6 kcal/mol), the synthesized compounds (6a-i) have shown high binding affinity and similar residual and DNA interaction profile with amino acid residues Asp-479, Ser-480, Glu-477, Ala-481, Arg-503, Gly-478, and Gly-504 and nucleic acid residues DT-8, DT-9, DG-10, DA-12, and DG-13. Compounds 6c and 6g have no hydrogen bonding interaction with amino acid residues within the binding pocket. The compounds 6a (–6.6 kcal/mol), 6b (–6.7 kcal/mol), and 6i (–6.5 kcal/mol) have shown better binding affinity and similar residual amino acid and DNA binding within the binding pockets of 3QX3 as compared to Vosaroxin (Figure 2). The *in silico* interaction results have shown that all the synthesized compounds (6a-i) have better binding affinity compared to Vosaroxin; among them compounds 6b (–6.7 kcal/mol) and 6f (–6.7 kcal/mol) revealed better binding affinity. The inhibition constant K_i values showed much better results for synthesized compounds 6a-i (0.726 to 3.493 nm) as compared to Vosaroxin (22.993 nm). Among them, 6b and 6f showed minimum value (0.726 nm), 6a was slightly higher (0.994 nm), and compound 6i showed more than 10-fold decrement (1.361 nm) to Vosaroxin (22.993 nm). Based on the molecular docking analysis results, all the synthesized compounds have shown comparable residual interactions and better docking scores than Vosaroxin (see supplementary materials (Figures S19–S28)). Hence, these compounds might prove to be better anticancer agents than Vosaroxin. The binding affinity, inhibition constant, H-bond, and residual interaction of all the synthesized compounds are summarized in Table 4.

3.2.2. Binding Mode of Analysis of Synthesized 1,8-Naphthyridine Derivatives Docked against E. coli DNA Gyrase B (PDB ID 6F86). DNA gyrase B, an enzyme belonging to a member of bacterial topoisomerase, controls the topology of DNA during transcription, replication, and recombination by introducing transient breaks to both DNA strands [60, 61]. Hence, the bacterial DNA gyrase is paramount for bacterial survival and therefore necessary to disrupt as an antibacterial drug target [62]. Therefore, in this study, the molecular docking analysis of the synthesized compounds was carried out to investigate their binding pattern with DNA gyrase and the results were compared with standard antibacterial agent (Ciprofloxacin). The synthesized compounds (6a-i) were found to have minimum binding energy ranging from –6.5 to –9.4 kcal/mol (Table 5), with the best result achieved using compound 6i (–9.4 kcal/mol). Compared to Ciprofloxacin, the synthesized compounds (6a-i) have shown high binding affinity (except 6d) and similar residual interaction profile with amino acid residues Glu-50, Gly-77, Ile-94, Ile-78, Pro-79, Ala-47, Thr-165, and H-bond with Asp-73, Arg-76, and Asn-46. All the synthesized ligands have revealed the crucial interaction between the ligand, Asp-73, and the water molecule with *E. coli* DNA gyrase B (6F86). It has been previously reported that binding modes between ligand, Asp-73, and water molecule are crucial for the inhibition for the DNA gyrase B [63]. Compounds 6a (Asp-49), 6b (Gly-77 and Thr-165), 6f (Glu-50), and 6i (Ala-47) have additional hydrogen bonding interaction with amino acid residues. The compounds 6c, 6d, 6e, 6g, and 6h have shown similar hydrogen bond (Gly-77) and residual amino acid binding within the binding pockets of 6F86 (Ile-78, Glu-50, Ile-94, and Pro-79). The *in silico* interaction results of the synthesized compounds (6a-i) showed better binding affinity in comparison with Ciprofloxacin; among them, compounds 6b (– 8.1 kcal/mol) and 6i (–9.4 kcal/mol) revealed the best binding affinity results. Compound 6d has shown smaller docking affinity (–6.5 kcal/mol) and partially matching amino acid residues interactions in comparison with Ciprofloxacin (Figure 3). The inhibition constant K_i values showed better results for synthesized compounds 6a-i (0.00015 to 1.36144 nm) as compared to Ciprofloxacin (0.08061 nm). Among them, 6i showed minimum value (0.00015 nm) and 6b was slightly higher (0.00895 nm), while 6h (0.02295 nm), 6a (0.03142 nm), and 6c (0.05888 nm) are comparable to Ciprofloxacin (0.08061 nm). Based on the molecular docking analysis results, all the synthesized compounds (except 6d) have shown comparable residual interactions and better docking scores than Ciprofloxacin (see supplementary materials (Figures S29–S38)). Therefore, these compounds might have potential to be promising antibacterial agents. The binding affinity, inhibition constant,

Table 3: Calculated green metrics for the scaled-up synthesis of 6-amino-4-(4-methoxyphenyl)-1-oxo-1, 2, 3, 4, 7a, 11b-hexahydro-4a1H-cyclopenta [b] indeno [1, 2, 3-de] [1,8] naphthyridine-4a1,7-dicarbonitrile [6c].

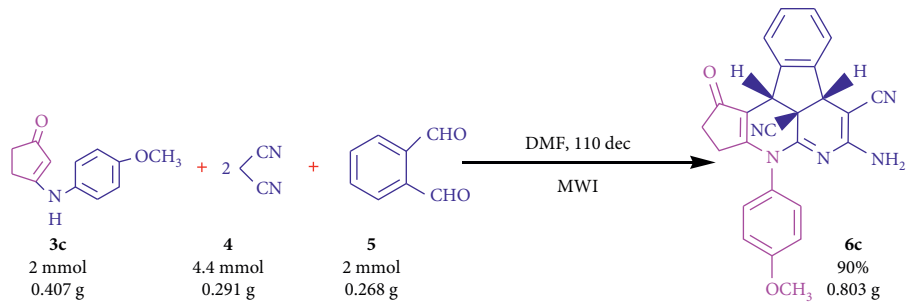

3c 2 mmol 0.407 g | **4** 4.4 mmol 0.291 g | **5** 2 mmol 0.268 g | **6c** 90% 0.803 g

Yield (%)	AE (%)	CE (%)	E-factor[a]	RME (%)	PMI
90	92.32	72.83	3.938	83.13	4.938

[a]calculation up to the crude product.

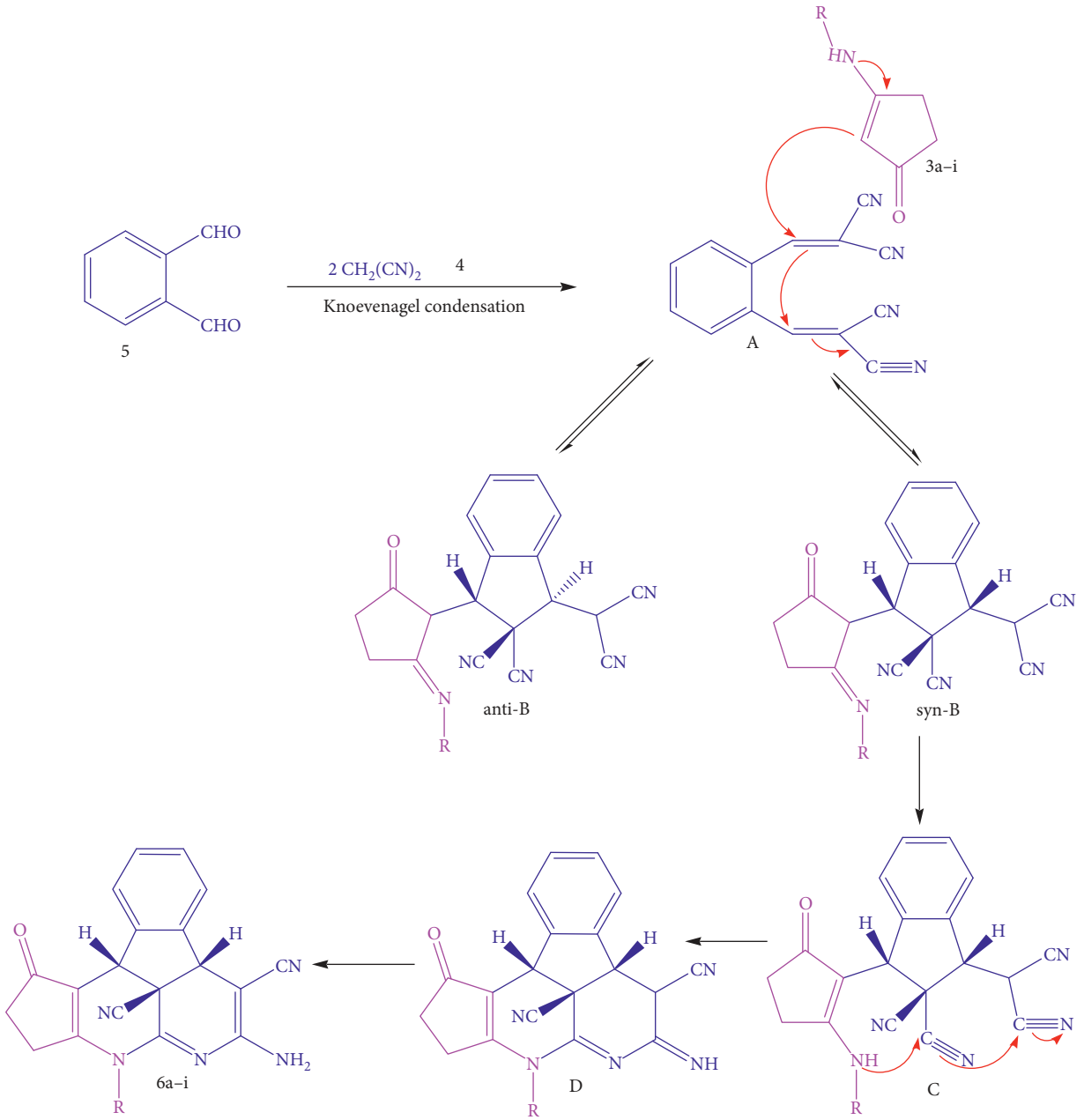

Scheme 3: Proposed mechanism for formation of compounds 6a-i.

Table 4: Molecular docking results of compounds 6a-i against human topoisomerase IIβ DNA (PDB ID 3QX3).

S. no.	Ligands	Binding affinity (kcal/mol)	Inhibition constant ki (nM)	Residual interactions			
				H-bond	DNA	Hydrophobic/cation-II	Van der Waals
6a	$C_{19}H_{13}N_5O$	−6.6	0.994	Asp-479, Ser-480	DT-8, DT-9, DG-10, DG-13	Glu-477	Gly-478, Leu-502, Arg-503, Gly-504, Tyr-821
6b	$C_{25}H_{17}N_5O$	−6.7	0.726	Ser-480, Gly-504	DT-8, DT-9, DG-13	—	Asp-479, Leu-502, Gly-776
6c	$C_{26}H_{19}N_5O_2$	−6.2	3.493	—	DT-8, DT-9, DG-10, DA-12, DG-13	Arg-503	Asp-479, Ser-480, Glu-477, Gly-478, Leu-502, Gly-504, Gly-776, Tyr-821
6d	$C_{26}H_{19}N_5O$	−6.3	2.551	Arg-503, Gln-778, Tyr-821	DT-8, DT-9, DG-10, DA-12, DG-13	—	Asp-479, Glu-477, Gly-504, Lys-505
6e	$C_{26}H_{19}N_5O$	−6.4	1.863	Gly-504	DT-8, DT-9, DA-12,	Arg-503	Asp-479, Ser-480, Gly-478, Leu-502, Gln-778, Gly-776
6f	$C_{27}H_{21}N_5O_2$	−6.7	0.726	Gln-778, Tyr-821	DT-8, DT-9, DG-10	Arg-503, Glu-477, Ala-481,	Asp-479, Ser-480, Gly-478, Asp-557
6g	$C_{26}H_{19}N_5OS$	−6.2	3.493	—	DT-8, DT-9, DG-10, DA-12	Arg-503	Asp-479, Ser-480, Glu-477, Gly-478, Gly-776, Leu-502, Gly-504, Tyr-821
6h	$C_{25}H_{16}BrN_5O$	−6.4	1.863	Gly-504	DT-8, DT-9, DA-12,	Arg-503	Ser-480, Glu-477, Gly-478, Leu-502, Tyr-821
6i	$C_{26}H_{16}F_3N_5O$	−6.5	1.361	Lys-505, Tyr-821	DT-8, DT-9, DA-12, DG-13	Gln-778	Arg-503, Gly-504
Vosaroxin	$C_{18}H_{19}N_5O_4S$	−5.6	22.993	Asp-479, Ser-480, Glu-477, Ala-481, Arg-503	DT-8, DT-9, DG-10, DA-12, DG-13	—	Gly-478, Gly-504

DA = deoxyadenosine; DG = deoxyguanosine; DT = deoxythymidine.

H-bond, and residual interaction of all the synthesized compounds are summarized in Table 5.

3.2.3. In Silico Pharmacokinetics (Drug-Likeness) and Toxicity Analysis. The drug-likeness of the synthesized 1,8-naphthyridine derivatives was characterized according to "Lipinski's rule of five." As per Lipinski's rule, the potential molecules should have the following physicochemical properties [64], such as (i) less than 5 hydrogen bond donors (HBDs), (ii) less than 10 hydrogen bond acceptors (HBAs), (iii) a molecular mass less than 500 Da, (iv) log P not greater than 5, and (v) total polar surface area (TPSA) which should not be >140 Å. The SwissADME computed results showed that all the synthesized compounds (6a-i) in the present study are satisfying Lipinski's rule of five with zero violations (Table 6) [65]. Hence, all the synthesized compounds might be candidates for anticancer and antimicrobial studies.

Evaluation of ADMET properties of newly synthesized compounds is pivotal in drug discovery [45]. The skin absorption of molecules is indicated by skin permeability value (Kp) in cm/s. The more negative the value of log K_p, the less the skin absorption [41, 66]. The skin permeability, K_p, values of all molecules (7.12 to −8.11 cm/s) are within the range of Vosaroxin (8.98 cm/s) inferring low skin permeability. In addition to that, absorption and distribution of drug molecules are measured by gastrointestinal (GI) and blood brain barrier (BBB) permeation. The SwissADME prediction parameters have shown that all the compounds 6a-h and 6i (except 6g) have high gastrointestinal (GI) absorption and none of the compounds have blood brain barrier (BBB) permeation. Drug metabolism has been mainly governed by a range of cytochromes (CYP's). Among them, CYP1A2, CYP2C19, CYP2C9, CYP2D6, and CYP3A4 are paramount for biotransformation of drug molecules [41]. SwissADME prediction has shown that all the compounds including Vosaroxin (except 6h) are substrates of permeability glycoprotein (P-gp). The prediction result exhibits that all the compounds are found to be noninhibitor for CYP2C19 and CYP2D6. The compounds 6b, 6d, 6e, 6h, and Vosaroxin are potential inhibitors for CYP1A2, and compounds 6a, 6c, 6f, 6g, and 6i are noninhibitors. For CYP2C9 and CYP3A4, the compounds 6a and Vosaroxin are noninhibitors, and the other compounds 6b-i are potential inhibitors. The *in silico* computed results of absorption, distribution, metabolism, and excretion (ADME) for synthesized compounds 6a-i and Vosaroxin are given in Table 7.

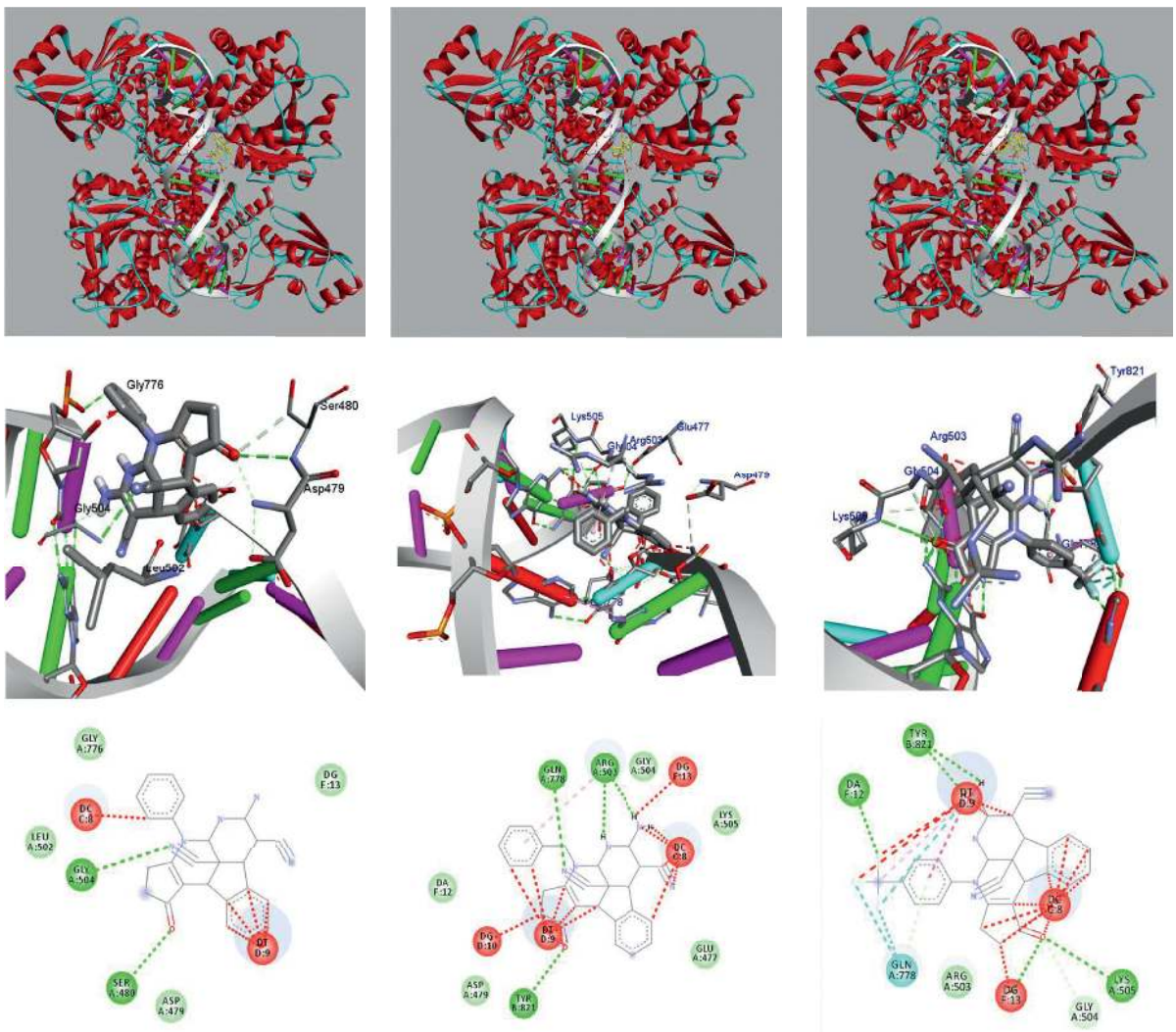

(a) (b) (c)

Figure 2: The 2D and 3D binding interactions of compounds 6b, 6d, and 6i (comparable to Vosaroxin) against human topoisomerase IIβ (PDB ID: 3QX3). 3D ribbon model shows the binding pocket structure of human topoisomerase IIβ with compounds. Hydrogen bonds between compounds and amino acids are shown as green-dashed lines, and hydrophobic interactions are shown as pink lines. (a) 6b, (b) 6d, and (c) 6i.

Table 5: Molecular docking results of compounds 6a-i against *E. coli* DNA gyrase B (PDB ID 6F86).

S. no.	Ligands	Binding affinity (kcal/mol)	Inhibition constant ki (nM)	H-bond	Residual interactions	
					Hydrophobic/cation-II	Van der Waals
6a	$C_{19}H_{13}N_5O$	−7.7	0.03142	Asp-49, Asn-46	Asp-73, Glu-50, Ile-94	Ile-78, Gly-77, Thr-165, Als-47, Asp-45
6b	$C_{25}H_{17}N_5O$	−8.1	0.00895	Asn-46, Gly-77, Thr-165	Arg-76, Pro-79, Glu-50	Asp-73, Asp-49, Ile-78, Ile-94
6c	$C_{26}H_{19}N_5O_2$	−7.5	0.05888	Gly-77	Ile-78, Ile-94, Glu-50, Pro-79	Asp-73, Asn-46, Asp-49, Arg-76, Arg-136, Thr-165
6d	$C_{26}H_{19}N_5O$	−6.5	1.36144	Gly-77	Ile-78, Arg-76, Glu-50	Asp-73, Asn-46, Ile-94, Arg-136, Thr-165
6e	$C_{26}H_{19}N_5O$	−7.7	0.03142	Gly-77	Ile-78, Ile-94, Pro-79, Glu-50	Asp-73, Asn-46, Asp-49, Arg-76, Arg-136, Thr-165
6f	$C_{27}H_{21}N_5O_2$	−7.3	0.11036	Asn-46, Glu-50	Arg-76, Pro-79	Asp-73, Gly-77, Ala-47, Asp-49, Thr-165, Gly-119, Val-120

Table 5: Continued.

S. no.	Ligands	Binding affinity (kcal/mol)	Inhibition constant ki (nM)	H-bond	Residual interactions	
					Hydrophobic/cation-II	Van der Waals
6g	$C_{26}H_{19}N_5OS$	−7.2	0.15108	Gly-77	Ile-78, Ile-94, Pro-79, Glu-50	Asp-73, Asn-46, Arg-76, Arg-136
6h	$C_{25}H_{16}BrN_5O$	−7.8	0.02295	Gly-77	Ile-78, Ile-94, Glu-50	Asp-73, Asn-46, Arg-76, Asp-49, Thr-165
6i	$C_{26}H_{16}F_3N_5O$	−9.4	0.00015	Ala-47	Asp-73, Asn-46, Ile-78, Asp49, Val-43	Arg-76, Thr-165, Val-167
Vosaroxin	$C_{18}H_{19}N_5O_4S$	−7.3	0.11036	Asp-73	Ile-78, Asn-46	Arg-76, Ala-47, Ile-94, Glu-50, Gly-77, Thr-165
Ciprofloxacin	$C_{17}H_{18}FN_3O_3$	−7.4	0.08061	Asp-73, Asn-46, Arg-76	Ile-78, Ile-94, Glu-50, Gly-77	Ala-47, Pro-79, Thr-165

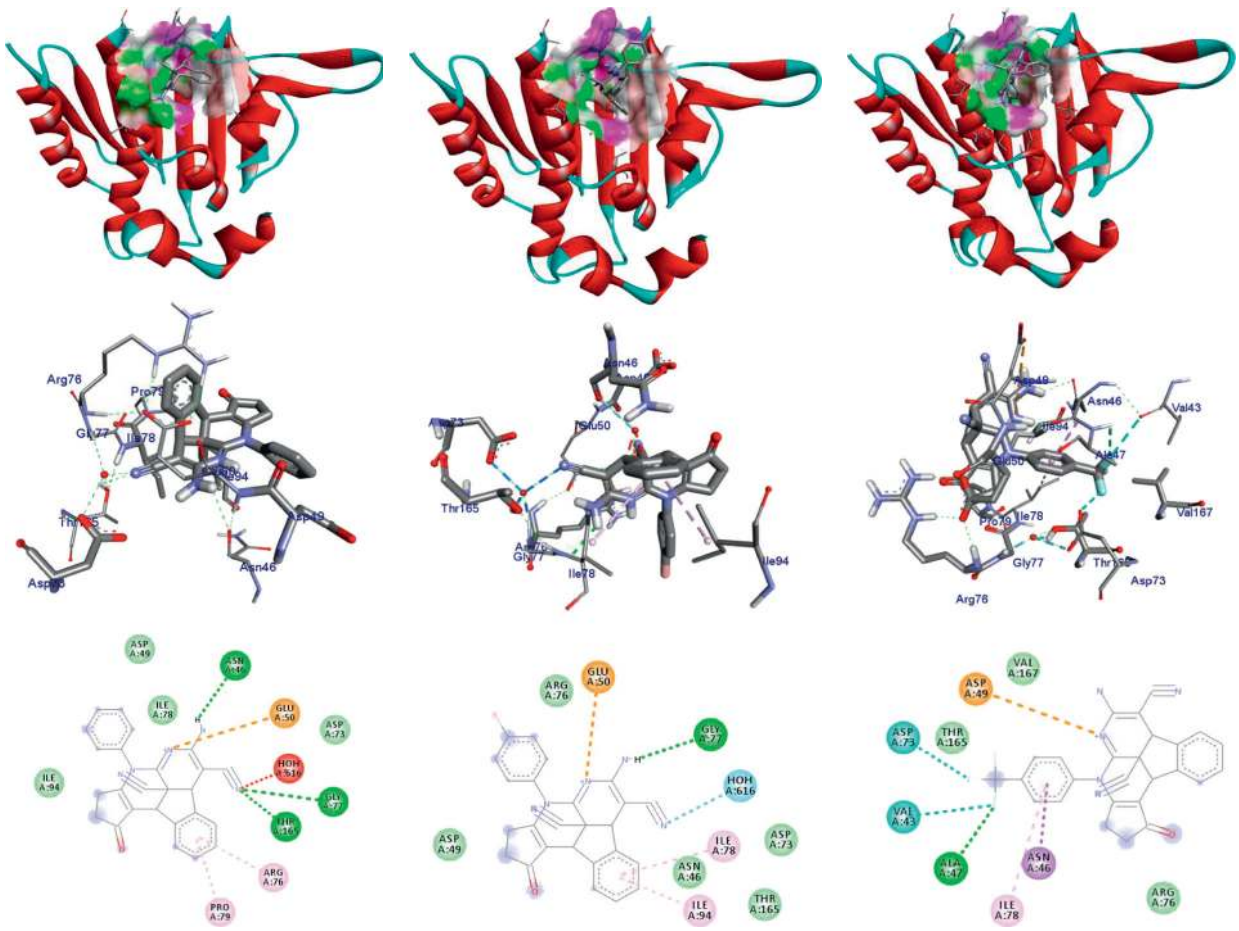

(a) (b) (c)

Figure 3: The 2D and 3D binding interactions of compounds 6b, 6h, and 6i (comparable to Ciprofloxacin) against *E. coli* DNA gyrase B (PDB ID: 6F86). 3D ribbon model shows the binding pocket structure of *E. coli* DNA gyrase B with compounds. Hydrogen bonds between compounds and amino acids are shown as green-dashed lines, and hydrophobic interactions are shown as pink lines. (a) 6b, (b) 6h, and (c) 6i.

Table 6: Drug-likeness predictions of compounds 6a-i, computed by SwissADME.

S. no.	Formula	Mol. Wt. (g/mol)	NHD	NHA	NRB	TPSA ($A^{°2}$)	LogP (cLogP)	Lipinski's rule of five with zero violations
6a	$C_{19}H_{13}N_5O$	327.34	2	4	0	115.06	1.58	0
6b	$C_{25}H_{17}N_5O$	403.44	1	4	1	106.27	2.36	0
6c	$C_{26}H_{19}N_5O_2$	433.46	1	5	2	115.50	2.66	0
6d	$C_{26}H_{19}N_5O$	417.46	1	4	2	106.27	2.52	0
6e	$C_{26}H_{19}N_5O$	417.46	1	4	1	106.27	2.54	0
6f	$C_{27}H_{21}N_5O_2$	447.49	1	5	3	115.50	2.71	0
6g	$C_{26}H_{19}N_5OS$	449.53	1	4	2	131.57	2.68	0
6h	$C_{25}H_{16}BrN_5O$	482.33	1	4	1	106.27	2.73	0
6i	$C_{26}H_{16}F_3N_5O$	471.43	1	7	2	106.27	2.65	0
Vosaroxin	$C_{18}H_{19}N_5O_4S$	401.45	2	9	5	136.13	0.963	0

NHD = number of hydrogen donors, NHA = number of hydrogen acceptors, NRB = number of rotatable bonds, and TPSA = total polar surface area.

Table 7: ADME predictions of compounds 6a-i, computed by SwissADME and PreADMET.

S. no.	Chemical formula	Skin permeation value (log kp) cm/s	GI absorption	BBB permeability	Inhibitor interaction (SwissADME/PreADMET)					
					P-gp substrate	CYP1A2 inhibitor	CYP2C19 inhibitor	CYP2C9 inhibitor	CYP2D6 inhibitor	CYP3A4 inhibitor
6a	$C_{19}H_{13}N_5O$	−8.11	High	No	Yes	No	No	No	No	No
6b	$C_{25}H_{17}N_5O$	−7.34	High	No	Yes	Yes	No	Yes	No	Yes
6c	$C_{26}H_{19}N_5O_2$	−7.54	High	No	Yes	No	No	Yes	No	Yes
6d	$C_{26}H_{19}N_5O$	−7.47	High	No	Yes	Yes	No	Yes	No	Yes
6e	$C_{26}H_{19}N_5O$	−7.16	High	No	Yes	Yes	No	Yes	No	Yes
6f	$C_{27}H_{21}N_5O_2$	−7.67	High	No	Yes	No	No	Yes	No	Yes
6g	$C_{26}H_{19}N_5OS$	−7.25	Low	No	Yes	No	No	Yes	No	Yes
6h	$C_{25}H_{16}BrN_5O$	−7.33	High	No	No	Yes	No	Yes	No	Yes
6i	$C_{26}H_{16}F_3N_5O$	−7.12	High	No	Yes	No	No	Yes	No	Yes
Vosaroxin	$C_{18}H_{19}N_5O_4S$	−8.98	High	No	Yes	Yes	No	No	No	No

GI = gastrointestinal, BBB = blood brain barrier, P-gp = P-glycoprotein, and CYP = cytochrome-P.

Table 8: Toxicity prediction of compounds 6a-i, computed by ProTox-II and OSIRIS property explorer.

S. no.	Formula	LD_{50} (mg/kg)	Toxicity class	Organ toxicity					
				Hepatotoxicity	Carcinogenicity	Immunotoxicity	Mutagenicity	Cytotoxicity	Irritant
6a	$C_{19}H_{13}N_5O$	500	4	Inactive	Inactive	Inactive	Active	Inactive	No
6b	$C_{25}H_{17}N_5O$	500	4	Inactive	Active	Inactive	Active	Inactive	No
6c	$C_{26}H_{19}N_5O_2$	500	4	Inactive	Active	Inactive	Inactive	Inactive	No
6d	$C_{26}H_{19}N_5O$	235	3	Inactive	Inactive	Inactive	Inactive	Inactive	No
6e	$C_{26}H_{19}N_5O$	500	4	Inactive	Active	Inactive	Active	Inactive	No
6f	$C_{27}H_{21}N_5O_2$	400	4	Inactive	Inactive	Inactive	Inactive	Inactive	No
6g	$C_{26}H_{19}N_5OS$	500	4	Active	Active	Inactive	Active	Inactive	No
6h	$C_{25}H_{16}BrN_5O$	500	4	Inactive	Inactive	Inactive	Inactive	Inactive	No
6i	$C_{26}H_{16}F_3N_5O$	500	4	Inactive	Inactive	Inactive	Inactive	Inactive	No
Vosaroxin	$C_{18}H_{19}N_5O_4S$	500	4	Active	Inactive	Inactive	Inactive	Inactive	No

Acute toxicity predictions result such as LD_{50} values and toxicity class classification [1 (toxic) to 6 (non-toxic)] reveals that none of the ligands have shown acute toxicity and were found to be similar to Vosaroxin. The synthesized compounds 6a-i have shown toxicity class classification 4 (harmful if swallowed). The toxicological prediction gives results of endpoints such as hepatotoxicity, carcinogenicity, mutagenicity, immunogenicity, and cytotoxicity. Compounds 6b, 6e, and 6i were predicted to be nonhepatotoxic, nonimmunotoxic, nonirritant, and noncytotoxic. However, the compounds 6b and 6e have shown carcinogenicity and mutagenicity. Among all the compounds, 6i was found to be completely nontoxic. ProTox-II and OSIRIS property explorer prediction analyses are shown in Table 8. Hence,

based on ADMET prediction analysis, compound 6i may be the better candidate compared to other synthesized compounds in the investigation.

4. Conclusions

In this investigation, we have developed a green synthetic procedure for the facile synthesis of various potentially biologically active hexahydro-4a1H-cyclopenta [b] indeno [1, 2, 3-de] [1,8] naphthyridine derivatives, based on a novel four-component domino reaction. Using this method, a diverse collection of 1,8-naphthyridine derivatives were rapidly constructed with excellent yields in short reaction times by simply heating a mixture of different enaminones, malononitrile, and *o*-phthalaldehyde in DMF, without a catalyst, under microwave irradiation. Furthermore, *in silico* molecular docking, drug-likeness, and ADMET studies while comparing with clinically proven drugs Vosaroxin and Ciprofloxacin revealed the possible potency of synthesized compounds towards anticancer and antimicrobial activities. Based on the molecular docking analysis results, all the synthesized compounds have shown better docking scores than Vosaroxin and Ciprofloxacin. Hence, these compounds might prove to be better anticancer agents than Vosaroxin and might have potential to be very good antibacterial agents. The SwissADME prediction results showed that all the synthesized compounds (6a-i) in the present study satisfy Lipinski's rule of five with zero violations. Better performing compounds 6b, 6e, and 6i were predicted to be non-hepatotoxic, nonimmunotoxic, nonirritant, and non-cytotoxic. However, the compounds 6b and 6e have shown carcinogenicity and mutagenicity. Compound 6i was found to be completely nontoxic. The result of the present investigation suggested that 6-amino-1-oxo-4-(4-trifluoromethyl)phenyl)-1, 2, 3, 4, 7a, 11b-hexahydro-4a1H-cyclopenta [b] indeno [1, 2, 3-de] [1,8] naphthyridine-4a1,7-dicarbonitrile (6i) may serve as a candidate that could be developed into potent human topoisomerase IIβ and *E. coli.* DNA gyrase B inhibitor. So, it is worthy to carry out further *in vitro*, *in vivo*, and preclinical studies of the most active compound to develop potent anticancer and antimicrobial agent. Based on the preliminary prediction results of this investigation, we are working on a new series of 1,8-naphthyridine derivatives to explore better structure activity relationship and to find out more potent, less toxic, and better biologically active scaffolds.

Data Availability

The Excel data used to support the findings of this study are available from the corresponding author upon request.

Conflicts of Interest

The authors declare that they have no conflicts of interest.

Acknowledgments

The authors are grateful to the management of Adama Science and Technology University, Adama, Ethiopia, for providing research facilities to this work.

Supplementary Materials

The supplementary materials contain experimental section, green metrics calculation, theory calculation of intermediate B, ^{1}H and ^{13}C NMR spectra of all the synthesized compounds (6a-i), the 2D and 3D binding interactions of Vosaroxin and all synthesized compounds (6a-i) against human topoisomerase IIβ (PDB ID: 3QX3), and the 2D and 3D binding interactions of Ciprofloxacin and all synthesized compounds (6a-i) against *E. coli* DNA gyrase B (PDB ID: 6F86). (*Supplementary Materials*)

References

[1] H.-R. Park, T. H. Kim, and K.-M. Bark, "Physicochemical properties of quinolone antibiotics in various environments," *European Journal of Medicinal Chemistry*, vol. 37, no. 6, pp. 443–460, 2002.

[2] V. K. Gurjar and D. Pal, "Design, in silico studies, and synthesis of new 1, 8-naphthyridine-3-carboxylic acid analogues and evaluation of their H1R antagonism effects," *RSC Advances*, vol. 10, no. 23, pp. 13907–13921, 2020.

[3] C. Masdeu, M. Fuertes, E. Martin-Encinas et al., "Fused 1, 5-naphthyridines: synthetic tools and applications," *Molecules*, vol. 25, no. 15, pp. 3508–3561, 2020.

[4] E. Kiselev, T. S. Dexheimer, Y. Pommier, and M. Cushman, "Design, synthesis, and evaluation of dibenzo [c, h] [1, 6] naphthyridines as topoisomerase I inhibitors and potential anticancer agents," *Journal of Medicinal Chemistry*, vol. 53, no. 24, pp. 8716–8726, 2010.

[5] V. Ravichandran, S. Shalini, K. Sundram, and A. D. Sokkalingam, "QSAR study of substituted 1, 3, 4-oxadiazole naphthyridines as HIV-1 integrase inhibitors," *European Journal of Medicinal Chemistry*, vol. 45, no. 7, pp. 2791–2797, 2010.

[6] N. E. Austin, M. S. Hadley, J. D. Harling et al., "The design of 8, 8-dimethyl [1, 6] naphthyridines as potential anticonvulsant agents," *Bioorganic & Medicinal Chemistry Letters*, vol. 13, no. 10, pp. 1627–1629, 2003.

[7] K. A. Roseman, M. M. Gould, W. M. Linfield, and B. E. Edwards, "Antimalarials. 8-chloro-4-(2'-N, N-dibutylamino-1'-hydroxyethyl) benzo [h]-1, 6-naphthyridine," *Journal of Medicinal Chemistry*, vol. 13, no. 2, pp. 230–233, 1970.

[8] J. Marco-Contelles, R. Leon, C. De Los Rios et al., "Tacripyrines, the first Tacrine–Dihydropyridine hybrids, as multitarget-directed ligands for the treatment of alzheimer's disease," *Journal of Medicinal Chemistry*, vol. 52, no. 9, pp. 2724–2732, 2009.

[9] A. Madaan, R. Verma, V. Kumar, A. T. Singh, S. K. Jain, and M. Jaggi, "1, 8-naphthyridine derivatives: a review of multiple biological activities," *Archiv Der Pharmazie*, vol. 348, no. 12, pp. 837–860, 2015.

[10] V. K. Gurjar and D. Pal, "Recent developments and multiple biological activities available with 1, 8-naphthyridine derivatives: a review," *International Journal of Pharmacy and Pharmaceutical Sciences*, vol. 11, pp. 17–37, 2019.

[11] G. Grossi, M. Di Braccio, G. Roma, V. Ballabeni, M. Tognolini, and E. Barocelli, "1, 8-naphthyridines v. novel N-substituted 5-amino-N, N-diethyl-9-isopropyl [1, 2, 4] triazolo [4, 3-a] [1, 8] naphthyridine-6-carboxamides, as potent anti-inflammatory and/or analgesic agents completely devoid of acute gastrolesivity," *European Journal of Medicinal Chemistry*, vol. 40, no. 2, pp. 155–165, 2005.

[12] S. Olepu, P. K. Suryadevara, K. Rivas et al., "2-oxo-tetrahydro-1, 8-naphthyridines as selective inhibitors of malarial protein farnesyltransferase and as anti-malarials," *Bioorganic & Medicinal Chemistry Letters*, vol. 18, no. 2, pp. 494–497, 2008.

[13] P. L. Ferrarini, C. Mori, M. Badawneh et al., "Synthesis of 1, 8-naphthyridine derivatives: potential antihypertensive agents-part VII," *European Journal of Medicinal Chemistry*, vol. 33, no. 5, pp. 383–397, 1998.

[14] A. A. Santilli, A. C. Scotese, R. F. Bauer, and S. C. Bell, "2-oxo-1, 8-naphthyridine-3-carboxylic acid derivatives with potent gastric antisecretory properties," *Journal of Medicinal Chemistry*, vol. 30, no. 12, pp. 2270–2277, 1987.

[15] P. L. Ferrarini, C. Mori, M. Badawneh et al., "Synthesis and antiplatelet activity of some 3-phenyl-1, 8-naphthyridine derivatives," *Il Farmaco*, vol. 55, no. 9-10, pp. 603–610, 2000.

[16] C. Kurumurthy, P. Sambasiva Rao, B. Veeraswamy et al., "A facile and single pot strategy for the synthesis of novel naphthyridine derivatives under microwave irradiation conditions using $ZnCl_2$ as catalyst, evaluation of AChE inhibitory activity, and molecular modeling studies," *Medicinal Chemistry Research*, vol. 21, no. 8, pp. 1785–1795, 2012.

[17] X. Huang, A. Zhang, D. Chen, Z. Jia, and X. Li, "4-substituted 4-(1H-1, 2, 3-triazol-1-yl) piperidine: novel C7 moieties of fluoroquinolones as antibacterial agents," *Bioorganic & Medicinal Chemistry Letters*, vol. 20, no. 9, pp. 2859–2863, 2010.

[18] J.-P. Surivet, R. Lange, C. Hubschwerlen et al., "Structure-guided design, synthesis and biological evaluation of novel DNA ligase inhibitors with in vitro and in vivo anti-staphylococcal activity," *Bioorganic & Medicinal Chemistry Letters*, vol. 22, no. 21, pp. 6705–6711, 2012.

[19] K. Tomita, Y. Tsuzuki, K.-I. Shibamori et al., "Synthesis and structure–activity relationships of novel 7-substituted 14-dihydro-4-oxo-1-(2-thiazolyl)-18-naphthyridine-3-carboxylic acids as antitumor agents. Part 1," *Journal of Medicinal Chemistry*, vol. 45, no. 25, pp. 5564–5575, 2002.

[20] L. Fu, X. Feng, J.-J. Wang et al., "Efficient synthesis and evaluation of antitumor activities of novel functionalized 1, 8-naphthyridine derivatives," *ACS Combinatorial Science*, vol. 17, no. 1, pp. 24–31, 2015.

[21] A. N. Al-Romaizan, T. S. Jaber, and N. S. Ahmed, "Novel 1, 8-naphthyridine derivatives: design, synthesis and in vitro screening of their cytotoxic activity against MCF7 cell line," *Open Chemistry*, vol. 17, no. 1, pp. 943–954, 2019.

[22] C. R. Nicoleti, D. N. Garcia, L. E. Da Silva et al., "Synthesis of 1, 8-naphthyridines and their application in the development of anionic fluorogenic chemosensors," *Journal of Fluorescence*, vol. 22, no. 4, pp. 1033–1046, 2012.

[23] J. A. Abbas and R. K. Stuart, "Vosaroxin: a novel antineoplastic quinolone," *Expert Opinion on Investigational Drugs*, vol. 21, no. 8, pp. 1223–1233, 2012.

[24] E. J. Walsby, S. J. Coles, S. Knapper, and A. K. Burnett, "The topoisomerase II inhibitor voreloxin causes cell cycle arrest and apoptosis in myeloid leukemia cells and acts in synergy with cytarabine," *Haematologica*, vol. 96, no. 3, pp. 393–399, 2011.

[25] S. Srivastava, A. Jha, S. Agarwal, R. Mukherjee, and A. Burman, "Synthesis and structure-activity relationships of potent antitumor active quinoline and naphthyridine derivatives," *Anti-Cancer Agents in Medicinal Chemistry*, vol. 7, no. 6, pp. 685–709, 2007.

[26] Y. J. Hwang, M. L. Chung, U. D. Sohn, and C. Im, "Cytotoxicity and structure-activity relationships of naphthyridine derivatives in human cervical cancer, leukemia, and prostate cancer," *The Korean Journal of Physiology & Pharmacology*, vol. 17, no. 6, pp. 517–523, 2013.

[27] N. Margiotta, S. Savino, V. Gandin, C. Marzano, and G. Natile, "Monofunctional platinum (II) complexes with potent tumor cell growth inhibitory activity: the effect of a hydrogen-bond donor/acceptor N-heterocyclic ligand," *ChemMedChem*, vol. 9, no. 6, pp. 1161–1168, 2014.

[28] P. T. Anastas and J. C. Warner, *Green Chemistry: Theory and Practical*, OUP, Cary, NC, USA, 2000.

[29] P. J. Dunn, A. S. Wells, and M. T. Williams, *Green Chemistry in Pharmaceutical Industry*, Wiley-VCH, Weinheim, Germany, 2010.

[30] G. Martinez-Ariza, M. Ayaz, F. Medda, and C. Hulme, "Synthesis of diverse nitrogen-enriched heterocyclic scaffolds using a suite of tunable one-pot multicomponent reactions," *The Journal of Organic Chemistry*, vol. 79, no. 11, pp. 5153–5162, 2014.

[31] G. Martinez-Ariza, M. Ayaz, S. A. Roberts, W. A. Rabanal-León, R. Arratia-Pérez, and C. Hulme, "The synthesis of stable, complex organocesium tetramic acids through the ugi reaction and cesium-carbonate-promoted cascades," *Angewandte Chemie International Edition*, vol. 54, no. 40, pp. 11672–11676, 2015.

[32] A. Dömling, W. Wang, and K. Wang, "Chemistry and biology of multicomponent reactions," *Chemical Reviews*, vol. 112, no. 6, pp. 3083–3135, 2012.

[33] R. A. Dongardive, A. K. Pande, S. V. Goswami, S. S. Pendalwar, and S. R. Bhusare, "A convenient one-pot three component synthesis of 1, 8-naphthyridine derivatives," *JETIR*, vol. 7, pp. 9–11, 2020.

[34] E. C. Anderson, H. F. Sneddon, and C. J. Hayes, "A mild synthesis of substituted 1, 8-naphthyridines," *Green Chemistry*, vol. 21, no. 11, pp. 3050–3058, 2019.

[35] L. W. Deady and D. M. Werden, "A convenient synthesis of pyrrolo [1, 2-a] quinoline-1, 5-diones and acridine-1, 9-diones," *Synthetic Communications*, vol. 17, no. 3, pp. 319–328, 1987.

[36] P. L. Ferrarini, C. Mori, O. Livi, G. Biagi, and A. M. Marini, "Synthesis of some substituted pyrido [1, 2-a] pyrimidin-4-ones and 1, 8-naphthyridines," *Journal of Heterocyclic Chemistry*, vol. 20, no. 4, pp. 1053–1057, 1983.

[37] E. M. Hawes and D. G. Wibberley, "1, 8-naphthyridines," *Journal of the Chemical Society C: Organic*, pp. 315–321, 1966.

[38] M. Kumar, T. Kaur, V. K. Gupta, and A. Sharma, "A green, catalyst-free, solvent-free, high yielding one step synthesis of functionalized benzo [f] furo [3, 2-c]chromen-4-(5H)-ones and furo [3, 2-c] quinolin-4-(5H)-ones," *RSC Advances*, vol. 5, no. 22, pp. 17087–17095, 2015.

[39] M. Kumar, S. Bagchi, and A. Sharma, "The first vinyl acetate mediated organocatalytic transesterification of phenols: a step towards sustainability," *New Journal of Chemistry*, vol. 39, no. 11, pp. 8329–8336, 2015a.

[40] A. Awasthi, M. Lohani, M. K. Singh, A. T. Singh, and M. Jaggi, "Pharmacokinetic evaluation of C-3 modified 1, 8-naphthyridine-3-carboxamide derivatives with potent anticancer activity: lead finding," *Journal of Enzyme Inhibition and Medicinal Chemistry*, vol. 29, no. 5, pp. 710–721, 2014.

[41] A. Daina, O. Michielin, and V. Zoete, "SwissADME: a free web tool to evaluate pharmacokinetics, drug-likeness and medicinal chemistry friendliness of small molecules," *Scientific Reports*, vol. 7, p. 42717, 2017.

[42] P. Banerjee, A. O. Eckert, A. K. Schrey, and R. Preissner, "ProTox-II: a webserver for the prediction of toxicity of

chemicals," *Nucleic Acids Research*, vol. 46, no. W1, pp. W257–W263, 2018.

[43] P. Banerjee, F. O. Dehnbostel, and R. Preissner, "Prediction is a balancing act: importance of sampling methods to balance sensitivity and specificity of predictive models based on imbalanced chemical data sets," *Frontiers in Chemistry*, vol. 6, p. 362, 2018.

[44] O. Trott, A. J. Olson, and A.D. Vina, "Improving the speed and accuracy of docking with a new scoring function, efficient optimization, and multithreading," *Journal of Computational Chemistry*, vol. 31, pp. 455–461, 2010.

[45] M. W. El-Saadi, T. Williams-Hart, B. A. Salvatore, and E. Mahdavian, "Use of in-silico assays to characterize the ADMET profile and identify potential therapeutic targets of fusarochromanone, a novel anti-cancer agent," *Silico Pharmacology*, vol. 3, p. 6, 2015.

[46] A. McCluskey, P. J. Robinson, T. Hill, J. L. Scott, and J. K. Edwards, "Green chemistry approaches to the Knoevenagel condensation: comparison of ethanol, water and solvent free (dry grind) approaches," *Tetrahedron Letters*, vol. 43, no. 17, pp. 3117–3120, 2002.

[47] M. Venkatanarayana and P. K. Dubey, "L-proline-catalyzed knoevenagel condensation: a facile, green synthesis of (E)-ethyl 2-cyano-3-(1H-indol-3-yl) acrylates and (E)-3-(1H-Indol-3-yl) acrylonitriles," *Synthetic Communications*, vol. 42, no. 12, pp. 1746–1759, 2012.

[48] E. V. Dalessandro, H. P. Collin, L. G. L. Guimarães, M. S. Valle, and J. R. Pliego, "Mechanism of the piperidine-catalyzed knoevenagel condensation reaction in methanol: the role of iminium and enolate ions," *The Journal of Physical Chemistry B*, vol. 121, no. 20, pp. 5300–5307, 2017.

[49] S. Khodabakhshi, B. Karami, K. Eskandari, and A. Rashidi, "A facile and practical p-toluenesulfonic acid catalyzed route to dicoumarols containing an Aroyl group," *South African Journal of Chemistry*, vol. 68, pp. 53–56, 2015.

[50] F. Zhang, Y.-X. Wang, F.-L. Yang, H.-Y. Zhang, and Y.-F. Zhao, "Efficient solvent-free knoevenagel condensation between β-diketone and aldehyde catalyzed by silica sulfuric acid," *Synthetic Communications*, vol. 41, no. 3, pp. 347–356, 2011.

[51] R. A. Hann, "Use of dimethylformamide as a solvent for the knoevenagel reaction," *Journal of the Chemical Society, Perkin Transactions 1*, vol. 1, pp. 1379-1380, 1974.

[52] S. Mallouk, K. Bougrin, A. Laghzizil, and R. Benhida, "Microwave-assisted and efficient solvent-free knoevenagel condensation. a sustainable protocol using porous calcium hydroxyapatite as catalyst," *Molecules*, vol. 15, no. 2, pp. 813–823, 2010.

[53] B. Trost, "The atom economy--a search for synthetic efficiency," *Science*, vol. 254, no. 5037, pp. 1471–1477, 1991.

[54] C. Jiménez-González, D. J. C. Constable, and C. S. Ponder, "Evaluating the "Greenness" of chemical processes and products in the pharmaceutical industry-a green metrics primer," *Chemical Society Reviews*, vol. 41, no. 4, pp. 1485–1498, 2012.

[55] X. Feng, Q. Wang, W. Lin, G.-L. Dou, Z.-B. Huang, and D.-Q. Shi, "Highly efficient synthesis of polysubstituted pyrroles via four-component domino reaction," *Organic Letters*, vol. 15, no. 10, pp. 2542–2545, 2013.

[56] C.-P. Cao, W. Lin, M.-H. Hu, Z.-B. Huang, and D.-Q. Shi, "Highly efficient construction of pentacyclic benzo [b] indeno-[1, 2, 3-de] [1, 8] naphthyridine derivatives via four-component domino reaction," *Chemical Communications*, vol. 49, no. 62, pp. 6983–6985, 2013.

[57] S. Cunha, W. Rodovalho, N. R. Azevedo, M. D. O. Mendonça, C. Lariucci, and I. Vencato, "The Michael reaction of enaminones with N-(p-tolyl)-maleimide: synthesis and structural analysis of succinimide-enaminones," *Journal of the Brazilian Chemical Society*, vol. 13, no. 5, pp. 629–634, 2002.

[58] C. Alonso, M. Fuertes, M. González, A. Rodríguez-Gascón, G. Rubiales, and F. Palacios, "Synthesis and biological evaluation of 1, 5-naphthyridines as topoisomerase I inhibitors. a new family of antiproliferative agents," *Current Topics in Medicinal Chemistry*, vol. 14, no. 23, pp. 2722–2728, 2014.

[59] C. Freeman, N. Keane, R. Swords, and F. Giles, "Vosaroxin: a new valuable tool with the potential to replace anthracyclines in the treatment of AML?" *Expert Opinion on Pharmacotherapy*, vol. 14, no. 10, pp. 1417–1427, 2013.

[60] R. Ziraldo, A. Hanke, and S. D. Levene, "Kinetic pathways of topology simplification by type-II topoisomerases in knotted supercoiled DNA," *Nucleic Acids Research*, vol. 47, no. 1, pp. 69–84, 2019.

[61] C. J. Dorman and M. J. Dorman, "DNA supercoiling is a fundamental regulatory principle in the control of bacterial gene expression," *Biophysical Reviews*, vol. 8, no. 3, pp. 209–220, 2016.

[62] Ž. Jakopin, J. Ilaš, M. Barančoková et al., "Discovery of substituted oxadiazoles as a novel scaffold for DNA gyrase inhibitors," *European Journal of Medicinal Chemistry*, vol. 130, pp. 171–184, 2017.

[63] S. Narramore, C. E. M. Stevenson, A. Maxwell, D. M. Lawson, and C. W. G. Fishwick, "New insights into the binding mode of pyridine-3-carboxamide inhibitors of *E. coli* DNA gyrase," *Bioorganic & Medicinal Chemistry*, vol. 27, no. 16, pp. 3546–3550, 2019.

[64] C. A. Lipinski, F. Lombardo, B. W. Dominy, and P. J. Feeney, "Experimental and computational approaches to estimate solubility and permeability in drug discovery and development settings[1]," *Advanced Drug Delivery Reviews*, vol. 46, no. 1-3, pp. 3–26, 2001.

[65] A. Ah and A. Yi, "In silico pharmacokinetics and molecular docking studies of lead compounds derived from Diospyros mespiliformis," *PharmaTutor*, vol. 7, no. 3, pp. 31–37, 2019.

[66] C.-P. Chen, C.-C. Chen, C.-W. Huang, and Y.-C. Chang, "Evaluating molecular properties involved in transport of small molecules in stratum corneum: a quantitative structure-activity relationship for skin permeability," *Molecules*, vol. 23, no. 4, pp. 911–927, 2018.